

# Growth Kinetics and Catalytic Effects in the Vapor Phase Epitaxy of Gallium Nitride

S. S. Liu\*<sup>1</sup> and D. A. Stevenson\*\*

Department of Materials Science and Engineering, Stanford University, Stanford, California 94305

## ABSTRACT

The kinetics of the heteroepitaxial film growth of GaN on sapphire by chemical vapor deposition was investigated under a variety of experimental conditions. The growth rate was observed to be linear with time for all conditions studied and was found to be significantly influenced by the following factors: composition of the reactants in the vapor, temperature in the reaction zone, substrate orientation, and dopant concentration. The Gibbs free energy change for the main deposition reaction was evaluated as a function of temperature and reactant composition using available thermochemical data and compared with the observed deposition rate. An apparent discrepancy between predicted and observed deposition rate was attributed to local differences in  $\text{NH}_3$  composition due to decomposition and/or to the uncertainty in available thermochemical data. Significant observations are reported concerning the decomposition kinetics of  $\text{NH}_3$  in different growth ambients.

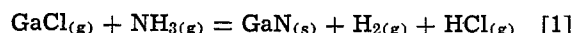
Gallium nitride (GaN), a III-V compound semiconductor, has a direct bandgap of 3.4 eV at room temperature (1, 2) and crystallizes in the wurtzite structure. Nominally pure GaN is invariably an n-type conductor with the carrier concentration in the  $10^{18}$ – $10^{19}$   $\text{cm}^{-3}$  range and resistivity in the  $10^{-2}$ – $10^{-3}$   $\Omega\text{-cm}$  range (3–7), the donors presumably being native defects such as nitrogen vacancies (3, 5, 8, 9) or gallium interstitials. Attempts to change the carrier type by p-type doping have been unsuccessful, presumably due to self-compensation; however, addition of group II elements such as Mg (3) and Zn produce insulating material (10–12). The large direct bandgap has prompted interest in this material for optoelectronic devices and recently GaN metal-insulator-semiconductor (MIS) light emitting diodes have been reported that emit violet (13), blue (10), green (11), and yellow (12) light. In addition, the piezoelectric properties and high acoustic velocities in this material make it attractive for acoustic devices (14). A major problem encountered in these device applications has been the quality of the material, particularly the reproducibility in the synthesis of material suitable for devices. The preparation of this material is an intriguing and challenging problem.

Gallium nitride is chemically inert but thermally unstable; GaN decomposes into the component elements prior to melting (15–18) (the normal decomposition temperature is  $\sim 800^\circ\text{C}$ ) and the high temperature and pressure for the coexistence of solid and liquid [estimated to be  $2000^\circ\text{C}$  and  $10^5$  atm (19)] make melt growth unfeasible. All practical methods for the synthesis of GaN utilize an active source of nitrogen, such as ammonia,  $\text{NH}_3$ . The most promising growth technique for device material has been the heteroepitaxial chemical vapor deposition utilizing  $\text{NH}_3$ , a vapor source of Ga (usually  $\text{GaCl}$ ), and a sapphire substrate. A significant feature of this process is the use of  $\text{NH}_3$  as an active nitrogen source under conditions where  $\text{NH}_3$  is thermodynamically unstable. Thus, factors influencing the kinetics of  $\text{NH}_3$  decomposition are highly relevant to this deposition process.

The present work was undertaken to interrelate the growth conditions, the growth kinetics, and the film characteristics for the heteroepitaxial deposition of GaN films. We present the following relevant observations and analyses: a development of the thermodynamics for the deposition reaction, measurements of the catalytic decomposition of  $\text{NH}_3$  in typical growth

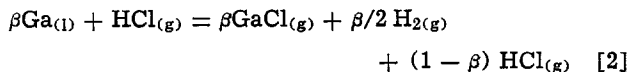
environments, and measurements of growth kinetics under a variety of experimental conditions. These experimental observations are discussed in terms of the optimum conditions for GaN film growth for device applications.

*Gallium nitride growth apparatus.*—A previous study (20) has established the main GaN deposition reaction to be



for the conditions used in the present investigation. The growth apparatus is a conventional hot wall open flow reactor and is diagrammed schematically in Fig. 1. The essential zones of the reactor are a source zone where  $\text{GaCl}_{(g)}$  is generated by passing  $\text{HCl}$  over Ga, a mixing zone where  $\text{GaCl}_{(g)}$  is mixed with  $\text{NH}_{3(g)}$ , and the deposition zone where the reaction mixture produces a deposit of GaN on the substrate as well as on the reactor walls. A sidearm, containing a crucible filled with Mg, is used to introduce Mg vapor into the mixing zone for the purpose of Mg doping. The temperature of the Mg source and the carrier gas flow rate determine the relative amount of Mg introduced. A stopcock and forechamber accommodate the introduction and withdrawal of the substrate without cooling the system to room temperature, thus facilitating several successive runs with a minimum of interruption. Palladium-diffused hydrogen was the carrier gas for all components. Thermocouples were used to monitor the temperature of the Mg source crucible and the substrate. Sapphire substrates of either basal plane orientation (0001) or R-plane orientation ( $1\bar{1}02$ ) were used. Further details of the process, such as specific temperatures and flow rates, are given in the discussion below and in a previous publication (13).

*Basic reaction.*—There are four reactions of central interest for the GaN deposition, two concerning the supply of reactants to the reaction chamber and two concerned, respectively, with the formation and depletion of GaN. The Ga source reaction is its conversion to  $\text{GaCl}$  by the reaction



where  $\beta$  is the conversion efficiency. At the temperature in question, the equilibrium conversion efficiency is essentially unity; however, the extent of attainment of equilibrium depends on several factors, principally the residence time of the  $\text{HCl}_{(g)}$  over the liquid Ga source, the Ga surface area, and the nature of the stir-

\* Electrochemical Society Student Member.

\*\* Electrochemical Society Active Member.

<sup>1</sup> Present address: Intel Corporation, Santa Clara, California 95051.

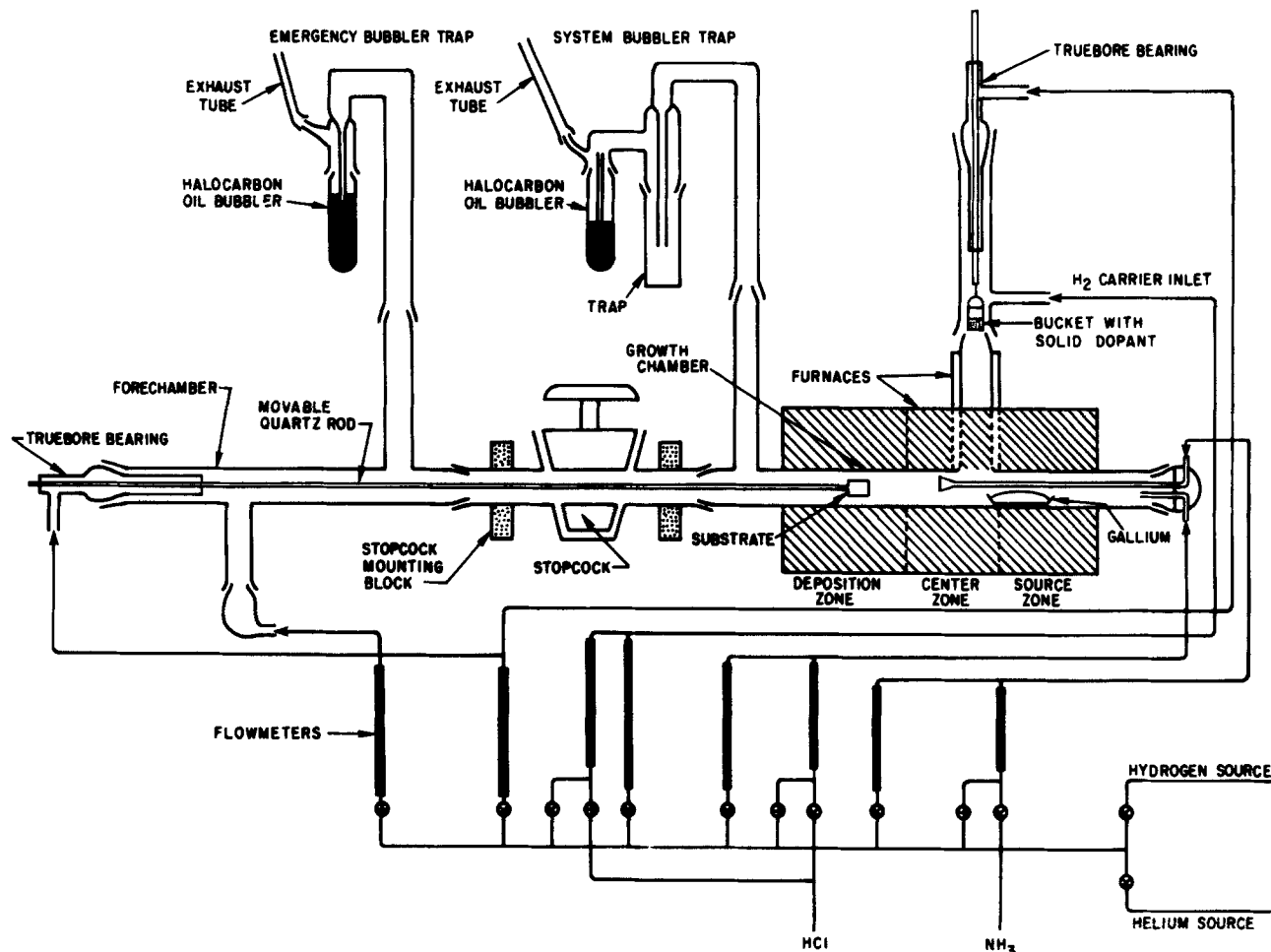
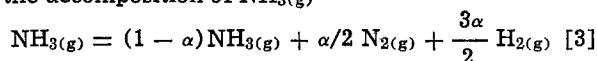
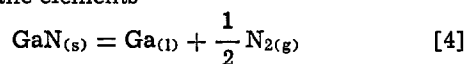


Fig. 1. Schematic diagram of the open-flow vapor growth system for preparing GaN

ring of the gaseous environment in the source zone. The other reaction that concerns the source of reactants is the decomposition of  $\text{NH}_3(\text{g})$



where  $\alpha$  is the degree of dissociation and is influenced principally by the temperature, partial pressure of  $\text{NH}_3(\text{g})$ , the residence time of  $\text{NH}_3$  in the reaction zone, and the catalytic nature of the environment in the reaction zone. The main formation reaction of GaN was given in Eq. [1]. As was already mentioned, GaN is unstable at elevated temperatures and tends to decompose into the elements



It is informative to compare the standard Gibbs free energy changes for the last three reactions, as given in Fig. 2. It is obvious from this figure that the decomposition of  $\text{NH}_3$  and GaN is overwhelmingly favored in the temperature regime of interest (growth temperatures ca. 1200°–1400°K). The fact that epitaxial growth actually occurs at these temperatures is a consequence of the sluggishness of the  $\text{NH}_3$  decomposition. It is appropriate to consider the influence of the extent of ammonia decomposition,  $\alpha$ , and the conversion efficiency to GaCl,  $\beta$ , on the driving force for the deposition reaction by applying the reaction isotherm to Eq. [1]

$$\Delta G = \Delta G^\circ + RT \ln(a_{\text{GaN}}a_{\text{HCl}}a_{\text{H}_2})/(a_{\text{GaCl}}a_{\text{NH}_3}) \quad [5]$$

where  $a$ 's are the activities of the different species denoted by the subscripts and  $\Delta G$  and  $\Delta G^\circ$  are the change in Gibbs free energy and the standard Gibbs free energy, respectively.

Assuming that the gaseous species are ideal and GaN is a pure phase, then

$$a_{\text{GaN}} = 1, \quad a_{\text{HCl}} = (1 - \beta)p_{\text{HCl}}, \quad a_{\text{GaCl}} = \beta p_{\text{HCl}}$$

$$a_{\text{H}_2} = p_{\text{H}_2} + \beta/2 p_{\text{HCl}} + 3\alpha/2 p_{\text{NH}_3}, \quad a_{\text{NH}_3} = (1 - \alpha)p_{\text{NH}_3}$$

The flow rate of HCl is much smaller than that of  $\text{NH}_3$  or  $\text{H}_2$ , or

$$p_{\text{HCl}} \ll p_{\text{NH}_3} p_{\text{H}_2}$$

and the total pressure is 1 atm, thus

$$p_{\text{H}_2} = 1 - p_{\text{NH}_3}$$

and we may write

$$\Delta G = \Delta G^\circ + RT \{ \ln(1 - \beta/\beta) + \ln[1 + (3\alpha/2 - 1)p_{\text{NH}_3}]/(1 - \alpha)p_{\text{NH}_3} \} \quad [6]$$

Here

$$\Delta G^\circ = (\Delta G^\circ_{\text{GaN}} + \Delta G^\circ_{\text{HCl}} + \Delta G^\circ_{\text{H}_2}) - (\Delta G^\circ_{\text{GaCl}} + \Delta G^\circ_{\text{NH}_3})$$

and  $\Delta G^\circ$ 's are the standard Gibbs free energy of formation for each species in question. Literature values for  $\Delta G^\circ$  as a function of  $T$  (in °K) are

$$\Delta G^\circ_{\text{GaN}} = 1.34 \times 10^{-2} T^2 - 15.27T + 1.48 \quad (15)$$

$$\Delta G^\circ_{\text{GaCl}} = 2.14 \times T \ln T - 29.42T - 1.68 \times 10^4 \quad (21)$$

$$\Delta G^\circ_{\text{HCl}} = 1.41 \times T \ln T - 12.71T - 2.08 \times 10^4 \quad (21)$$

with  $\Delta G^\circ_{\text{H}_2} = 0$  and  $\Delta G^\circ_{\text{NH}_3}$  tabulated in the JANAF table (22).

$\Delta G^\circ$  and  $\Delta G$  can therefore be plotted as a function of  $T$  with different values of  $\alpha$  and  $\beta$ , as shown in Fig. 3 and 4. As can be seen in these figures,  $\Delta G^\circ$  and all  $\Delta G$ 's go through a maximum as temperature changes. The peak shifts toward the lower temperature side with decreased value as either  $\alpha$  increases or  $\beta$  decreases. This indicates the existence of an optimum temperature as far as the local thermodynamic affinity is concerned. The broken lines in the figures indicate the temperature regime commonly used for growth.

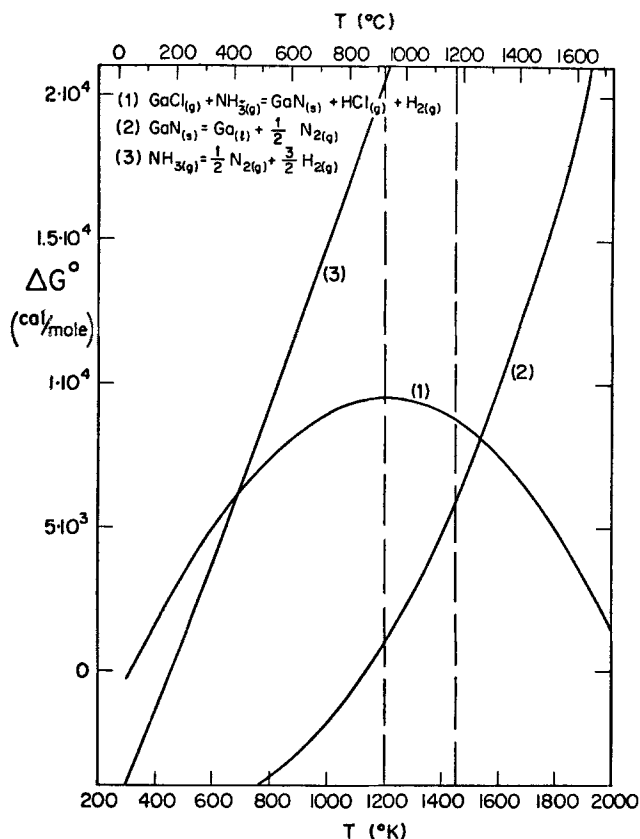


Fig. 2. Plot of  $\Delta G^\circ$  vs.  $T$  for three possible reactions in the deposition zone.

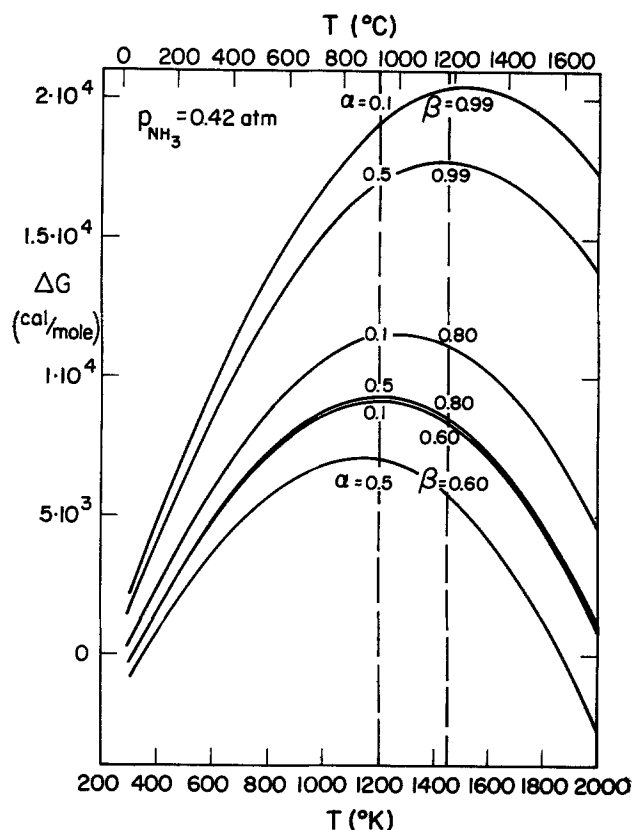


Fig. 4. Plot of  $\Delta G$  vs.  $T$  for  $p_{\text{NH}_3} = 0.42$  atm

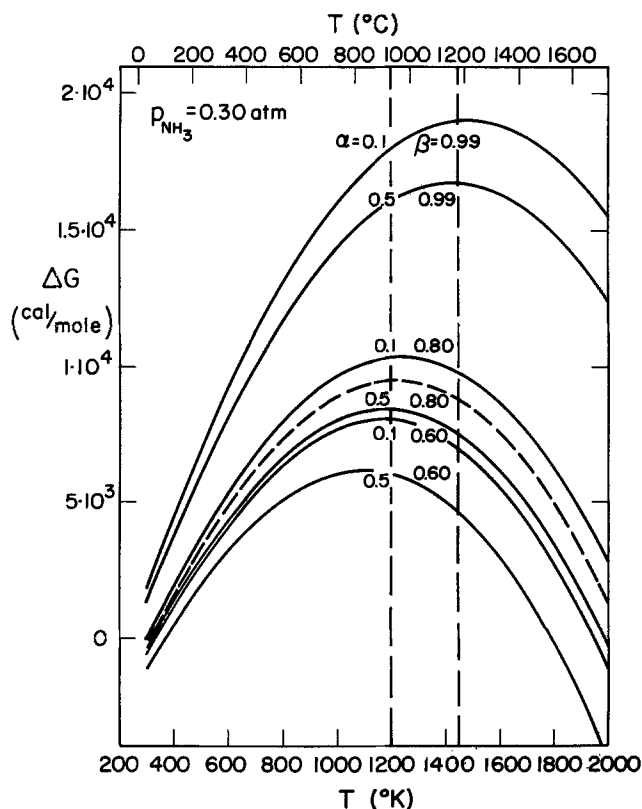


Fig. 3. Plot of  $\Delta G$  vs.  $T$  for  $p_{\text{NH}_3} = 0.30$  atm

It should be noted that the affinity in question is the initial affinity and as the reaction proceeds the concentration of HCl increases and causes the affinity to decrease in accord with Eq. [5].

#### Experimental

It is obvious from the foregoing discussion that the concentrations of  $\text{GaCl}_{(g)}$  and  $\text{NH}_{3(g)}$  are key factors

in determining the basic thermodynamic driving force for the deposition reaction. Hence, factors affecting their concentration will certainly influence the nature of the GaN deposit. In this section we describe the techniques that were employed to study the conversion efficiency of  $\text{Ga}_{(l)}$  to  $\text{GaCl}_{(g)}$  and the parameters involved in the decomposition of  $\text{NH}_3$ . In addition, we describe techniques that were used to measure the growth rate of the deposits under a variety of experimental conditions.

**Determination of the Ga-GaCl conversion and the extent of  $\text{NH}_3$  decomposition.**—Both the Ga-GaCl conversion and the extent of  $\text{NH}_3$  decomposition were accomplished by a straightforward acid-base titration technique. For all determinations, the actual growth system was used (Fig. 1) with the addition of a manometer connected to the sidearm to monitor the pressure of the system and the addition of a series of three traps at the outlet to trap the effluent gases for analysis. The three traps were used to ensure that there was complete trapping of the gas in question. The conditions of temperature, gas composition, and gas flow rates spanned the range of interest for the actual epitaxial growth procedure. In the case of the Ga-GaCl conversion, a mixture of HCl and  $\text{H}_2$  gases was flowed over the Ga boat in the source zone and the unreacted HCl collected in a series of three aqueous traps. The total HCl collected was determined by titration with a standard 0.1N NaOH solution. The actual HCl flow rates were checked by running the experiment without the presence of Ga, thus, no conversion of the HCl. A cross check on the Ga-GaCl conversion was obtained by measurement of the weight loss of the Ga boat in the source zone. In the case of the  $\text{NH}_3$  decomposition study, the approach was similar except that in this case a  $\text{NH}_3$ - $\text{H}_2$  gas mixture, after passing through the furnace, was passed through a series of traps containing HCl; the first trap contained a standardized 5N HCl and the second and third 1N HCl. The respective flow rates of  $\text{NH}_3$  and  $\text{H}_2$  were 1060 and 1440 ml/min and the back pressure caused by the traps was approximately 0.8 psi, a pressure well below the level corre-

sponding to any significant leak rate. The amount of  $\text{NH}_3$  trapped was determined by titration of the remaining HCl in all three traps using a standard 1N NaOH solution. In these experiments, an appreciable amount of time was allowed for the system to reach a steady state before sampling of the effluent was begun. The NaOH and the HCl solutions were standardized using potassium biphthalate weighed on a Mettler microbalance. The indicators used in the standardization and the HCl titration were *o*-cresolphthalein and methyl red, respectively. Similar to the HCl case, the actual flow of  $\text{NH}_3$  was checked by flowing the gases through a cold furnace under conditions such that no decomposition would occur.

**Growth rate determination.**—The growth of GaN was determined by weighing the sapphire substrate on a Mettler microbalance prior to and subsequent to the GaN deposition for a given time of deposition with specified deposition conditions. The growth rate, expressed in terms of micrometers per minute was obtained by converting the weight gain to thickness. The latter assumption was justified as reasonable by observations of the deposit using both optical and scanning electron microscopy. The growth rate was also determined by direct thickness measurements by fracturing the sample and viewing the layer in cross section with a vernier lens, using optical microscopy.

### Experimental Results

**Conversion efficiency of HCl to GaCl ( $\beta$ ) and the extent of decomposition of  $\text{NH}_3$  ( $\alpha$ ).**—The quantities  $\beta$  and  $\alpha$  are essential for the prediction of the affinity of the main deposition reaction and were determined for a variety of experimental conditions in the range of interest for actual deposition systems. Figure 5 shows the results of the determination of the HCl conversion efficiency as a function of the HCl flow rate at a temperature of 950°C. As expected, the conversion efficiency decreases as the flow rate increases, presumably due to a decreased residence time. For the highest flow rate studied, the conversion efficiency was ~97% as compared with ~99% for the slowest flow rate (which was ~1/10 of the maximum). Thus, for all the conditions used in the present study, the conversion may be regarded as complete.

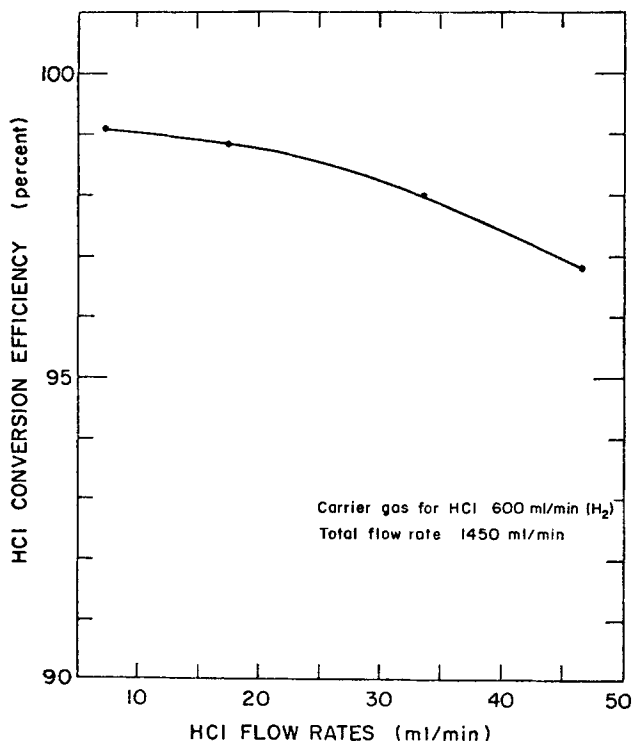


Fig. 5. Plot of the HCl conversion efficiency vs. HCl flow rates for a temperature of 950°C.

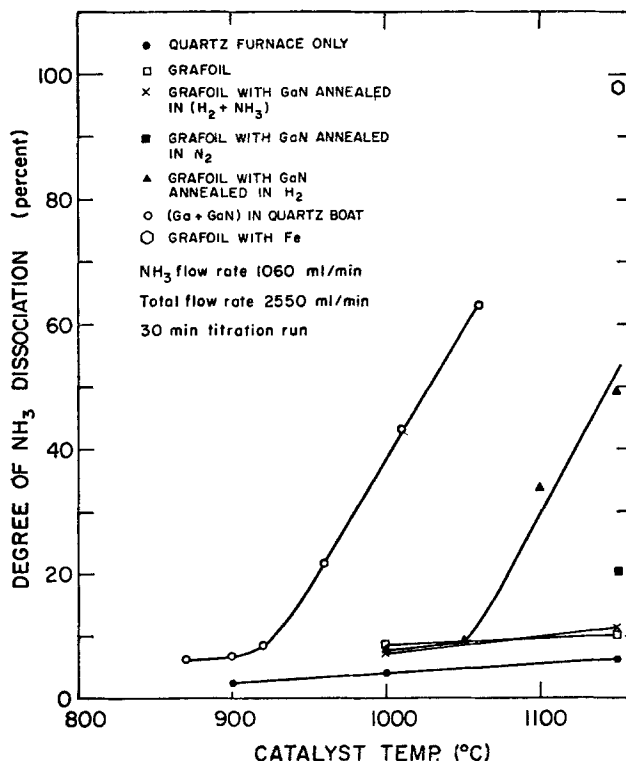


Fig. 6. Plot of the degree of  $\text{NH}_3$  decomposition vs. the temperature of different catalytic environments prepared in the growth furnace.

The degree of  $\text{NH}_3$  dissociation was determined as a function of temperature for several different environments and the results are summarized in Fig. 6. As shown by this figure, if the  $\text{NH}_3$  contacts only pure quartz tubes (vitrified or devitrified) or a new graphite liner (Grafoil) the degree of dissociation is linear with temperature and ranges between 2 and 6 and 5 and 10%, respectively, for the temperature interval of 900°–1150°C. If, however, GaN is predeposited on the Grafoil liner, the thermal history of the liner becomes important. When the predeposited GaN was annealed in an ambient of  $\text{NH}_3$  sufficient to prevent decomposition of GaN, the extent of decomposition was the same as for the pure graphite environment. When GaN is annealed in pure  $\text{N}_2$  or pure  $\text{H}_2$  prior to exposure to  $\text{NH}_3$ , a significant enhancement in  $\alpha$  occurs at elevated temperatures, with an apparent threshold temperature of ~1050°C for the  $\text{H}_2$  annealing case. To ascertain the reason for the enhanced catalytic effect and the significance of an apparent threshold temperature, the surfaces of GaN were examined by scanning electron microscopy (SEM) after appropriate anneals and the results are shown in Fig. 7. After annealing in a pure  $\text{H}_2$  ambient at 1000°C for 1 hr, the appearance of Ga droplets due to the decomposition is easily detected. Subsequent annealing in a  $\text{NH}_3$ -containing ambient results in a uniform texture if annealing is carried out at a temperature below the threshold temperature, presumably due to the reformation of GaN from the Ga droplets. By contrast the droplets will persist if the annealing with  $\text{NH}_3$  is performed above the threshold temperature. The supposition of the presence of Ga in the SEM micrographs was confirmed using x-ray diffraction. Since GaN itself was shown to have little influence on the decomposition of  $\text{NH}_3$ , there are two possible reasons for the anomalous enhancement in the catalytic decomposition of  $\text{NH}_3$  caused by the partial decomposition of GaN: the presence of pure liquid Ga, or the coexistence of Ga-GaN.

To determine the role of liquid Ga, a sample of pure Ga was placed in a boat located at the  $\text{NH}_3$  inlet. There was no significant influence on the  $\text{NH}_3$  decomposition for temperatures below 1000°C and a thin coat

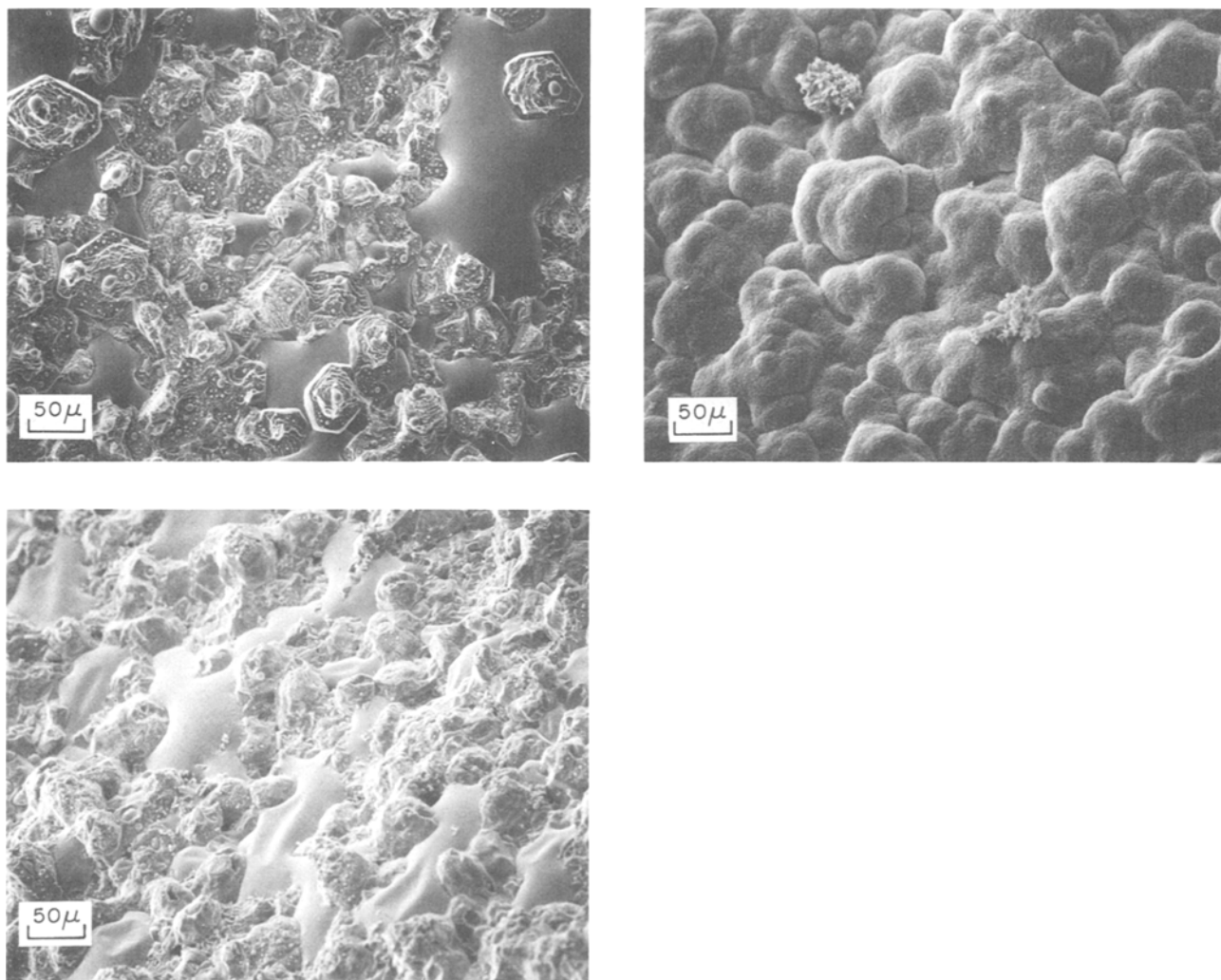


Fig. 7. Secondary emission micrographs of GaN-predeposited Grafoil liner: (a, left) after annealing in  $H_2$ -only ambient for 1 hr at about  $1000^\circ C$  after passing  $NH_3$  through the liner shown in (a) for 30 min; (b, right) at temperatures below the "threshold" point; and (c, bottom) at temperatures above the "threshold" point.

of GaN formed on the Ga. Above  $1025^\circ C$ , however, a dramatic change occurred; significantly more  $NH_3$  was decomposed and the Ga reacted to form a large amount of dark gray spongy material which filled the tube but did not block the gas flow. Between  $1000^\circ$  and  $1025^\circ C$ , a golden spongy material was generally formed with no enhancement in the extent of  $NH_3$  decomposition. The fact that pure Ga reacts with  $NH_3$  at all temperatures investigated implies that it does not decompose  $NH_3$  rapidly, otherwise  $NH_3$  would not be available for the formation of GaN.

The material obtained above  $1025^\circ C$  was analyzed by x-ray diffraction and by chemical analysis. It was found to be a conglomerate containing about 60% Ga and 40% GaN in polycrystalline form. The SEM micrographs of this material, Fig. 8, demonstrated the general porosity of the materials (Fig. 8a) which was the result of the formation of numerous fine dendritic crystallites (Fig. 8b). The Ga in the conglomerate was removed with aqua regia exposing micrometer-sized GaN dendrites (Fig. 8c). The catalytic nature of this conglomerate material was investigated by placing a sample near the  $NH_3$  inlet and performing the titration analysis as previously described. The results, shown in Fig. 6, show a similar behavior to the hydrogen-annealed GaN material except that the "threshold" temperature is lower. This confirms that the co-existence of Ga and GaN has a significant catalytic effect for the decomposition of  $NH_3$ . The lower threshold temperature for the conglomerate material is presumably the result of more total surface area.

For comparison purposes, the catalytic activity of a well-known catalyst for  $NH_3$  decomposition was evaluated in our system. The catalyst was fine Fe particles obtained by decomposition of  $FeCl_3$  on Grafoil in a hydrogen ambient and caused virtually complete decomposition of the  $NH_3$  at  $1150^\circ C$ , as seen from Fig. 6, and it is known that this catalyst is of comparable effectiveness at lower temperatures as well. It must be emphasized that the GaN-Ga conglomerate would not be an effective commercial catalyst for ammonia synthesis; however, its catalytic effect would certainly influence the chemical vapor deposition of GaN.

**Growth rate studies.**—The growth rate of heteroepitaxial GaN depends on the following parameters: the growth temperature, the flow rate of reactants, substrate orientation, growth environment, and Mg-doping.

To study the influence of these growth variables, different temperature profiles, providing growth temperatures within the range of interest as indicated in Fig. 2-4, were investigated and two representative profiles selected for more extensive examination. The results are summarized in Fig. 9 and 10 for average temperatures of  $1050^\circ$  and  $950^\circ C$ , respectively. The modest increase in the furnace temperature during actual growth (the dashed curve) as compared to the profile when only  $H_2$  carrier gas is passed through the furnace (the solid curve) is attributed to the exothermic nature of the reaction. Since it was established that the growth rate is linear, for given growth conditions (Fig. 11), the growth rate for each individual condition may

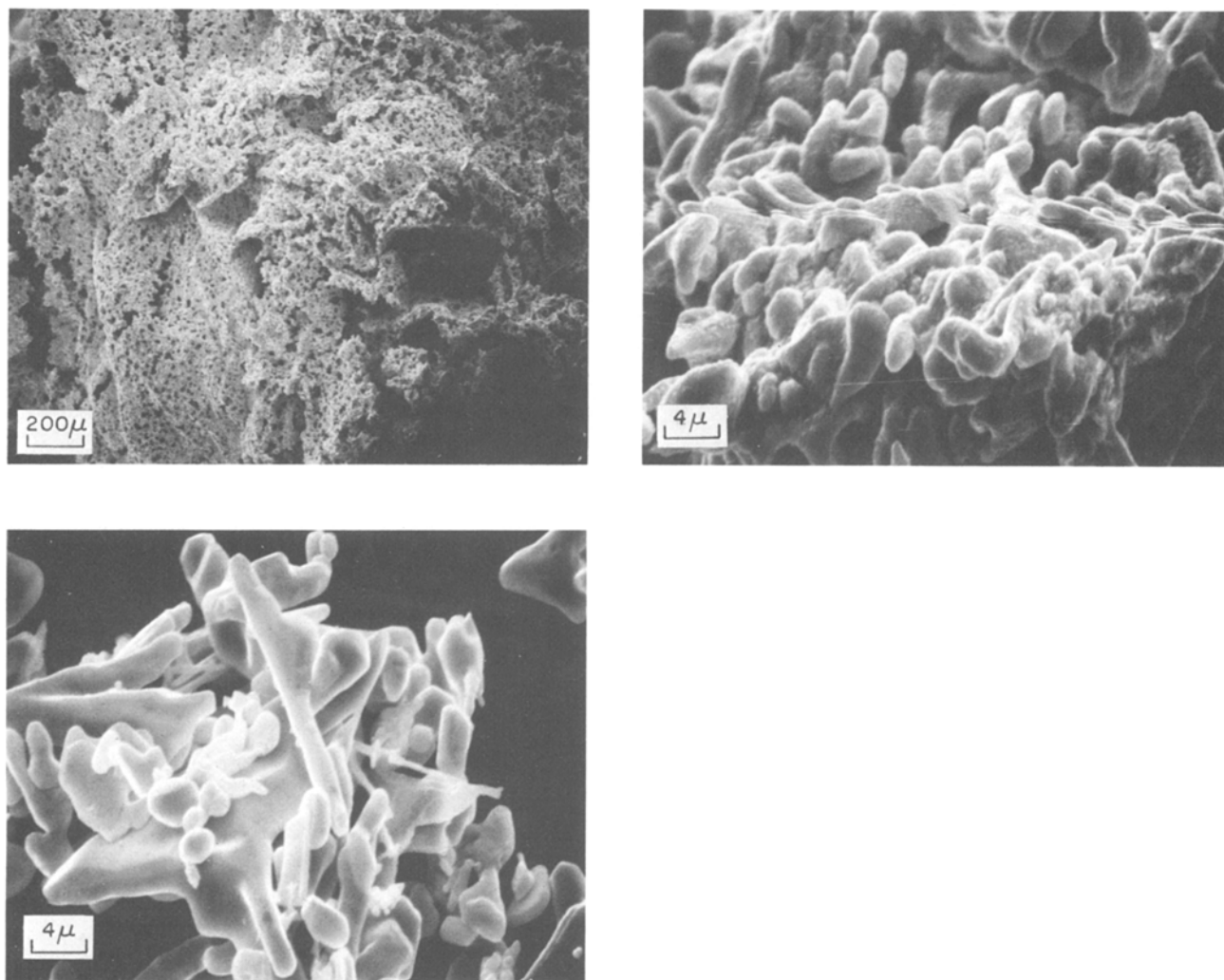


Fig. 8. Secondary emission micrographs of Ga-GaN mixture: (a, left) at 50 $\times$ ; (b, right) at 2500 $\times$ ; and (c, bottom) at 2500 $\times$ , after removing Ga.

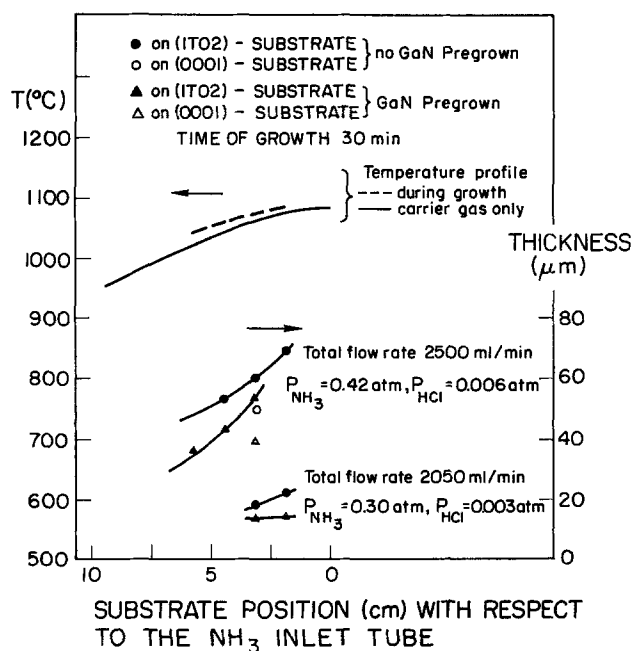


Fig. 9. Plot of growth temperature ( $>1000^{\circ}\text{C}$ ) and undoped GaN layer thickness vs. substrate position.

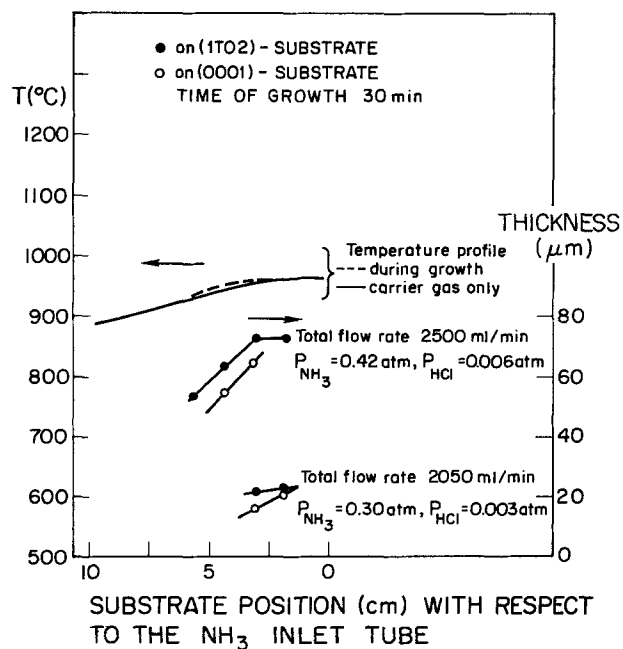


Fig. 10. Plot of growth temperature ( $<1000^{\circ}\text{C}$ ) and undoped GaN layer thickness vs. substrate position.

be obtained from the layer thickness after 30 min of growth. Several important trends that are apparent from these graphs may be summarized as follows:

(i) *Growth temperature.*—Comparison of identical substrate positions for the high and low temperature cases established that the growth rate decreases with

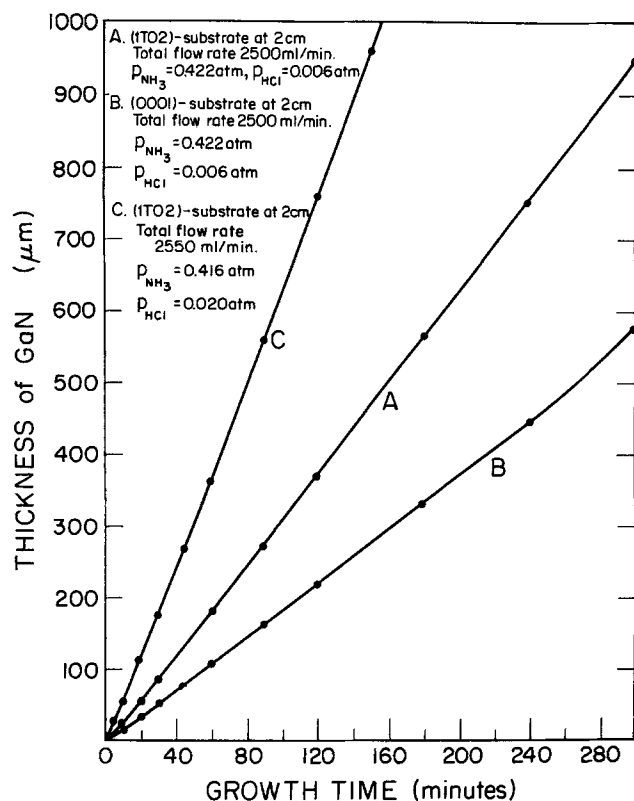


Fig. 11. Plot of undoped GaN layer thickness vs. growth time

increasing temperature within the temperature regime of interest for both R-plane and basal-plane substrates. The temperature gradient at a specific growth site is generally not a major factor unless it is extremely shallow or steep. For shallow gradients, the heat of reaction is not conducted away as rapidly and the temperature increases as growth proceeds with a consequent influence on the growth rate and the surface morphology. For steep gradients, there is evidence of a homogeneous reaction in the gas stream prior to the heterogeneous reaction at the substrate.

(ii) *Flow rate.*—The influence of gas flow rate concerns the total flow rate, the carrier gas flow rate, and the flow rates of the reactant gases ( $\text{HCl}$  and  $\text{NH}_3$ ). The influence of changing the individual reactant gas flow rates was most extensively studied. The results for two sets of  $\text{NH}_3$  and  $\text{HCl}$  flow rates, with the hydrogen carrier gas flow rate kept constant, are shown in Fig. 9 and 10, and the influence of varying individual reactant gas flow rate is described in Fig. 11 and 12. It is evident that the growth rate increases with increasing flow rates of the reactant gases if either one or both rates are increased.

(iii) *Substrate position.*—As shown in Fig. 9 and 10, the growth rate decreases as the substrate position is moved downstream from the  $\text{NH}_3$  inlet, presumably due to the depletion of the reactant species caused by deposition on the Grafoil liner prior to encountering the substrate.

(iv) *Substrate orientation.*—The growth rate on the (1102) or R-plane orientation was observed to be greater than that on the (0001) or basal-plane orientation for all the conditions investigated in this study, as shown in Fig. 9–12.

(v) *Growth environment.*—The enhanced  $\text{NH}_3$  decomposition caused by the coexistence of Ga–Ga<sub>2</sub>N, as described in the previous section, has a direct influence on the growth rate at temperatures where part of the system is above the threshold temperature of  $\sim 1000^\circ\text{C}$  for enhanced ammonia decomposition (cf. Fig. 6). Thus, for the higher temperature series, described in Fig. 9, there is a significant decrease in the growth rate if the growth environment includes Ga–Ga<sub>2</sub>N co-

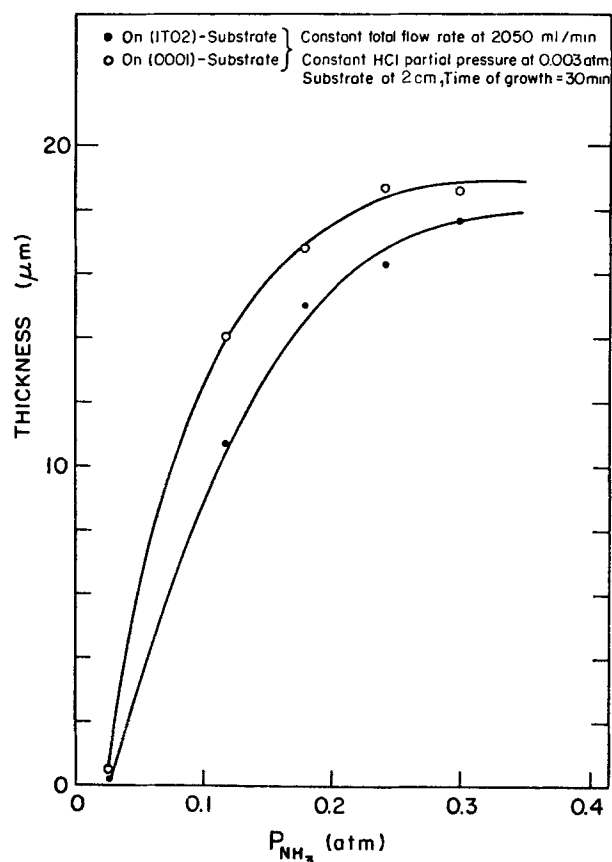


Fig. 12. Plot of undoped GaN layer thickness vs.  $p_{\text{NH}_3}$  for constant  $p_{\text{GaCl}}$ .

existence, as the result of the annealing of pregrown GaN in a  $\text{H}_2$  ambient. For the low temperature series, however, where there is no part of the system above the threshold temperature (Fig. 10), there is no difference observed for two different growth environments.

(vi) *Mg-doping.*—A previous study (1) had shown that the rate of GaN deposition was lower during Mg doping than during growth prior to the doping. This implied that either Mg doping retarded the growth rate or the growth rate was not linear with time (i.e., the growth rate was smaller at later times when Mg doping was occurring). The present study has established that the growth rate of the undoped layer is linear with time, thus Mg doping must decrease the growth rate. This decrease was established experimentally, with the results shown in Fig. 13. As can be seen from this graph, there is a substantial decrease in growth rate for either substrate orientation as the partial pressure of the Mg (as controlled by the temperature of the Mg reservoir) is increased in the growth system.

## Discussion

*Catalytic effect.*—It has been established in this study that the growth environment can significantly influence the extent of  $\text{NH}_3$  decomposition; limited decomposition occurs in quartz and graphite environments (up to  $\sim 10\%$ ) whereas more extensive decomposition occurs (up to  $\sim 60\%$ ) above a threshold temperature of  $950^\circ\text{--}1050^\circ\text{C}$  if Ga and GaN coexist. It is appropriate to compare these results with previous investigations and to speculate on the causes and implications of this behavior. Other workers (20, 23) have reported that graphite and devitrified quartz exhibit catalytic effects for  $\text{NH}_3$  decomposition in various vapor growth systems. As established in the present study, however, their influence is relatively modest compared to the Ga–Ga<sub>2</sub>N mixture. Recently, Raman spectroscopy has been applied to profile the  $\text{NH}_3$  composition in the vicinity of a graphite susceptor in a CVD system and



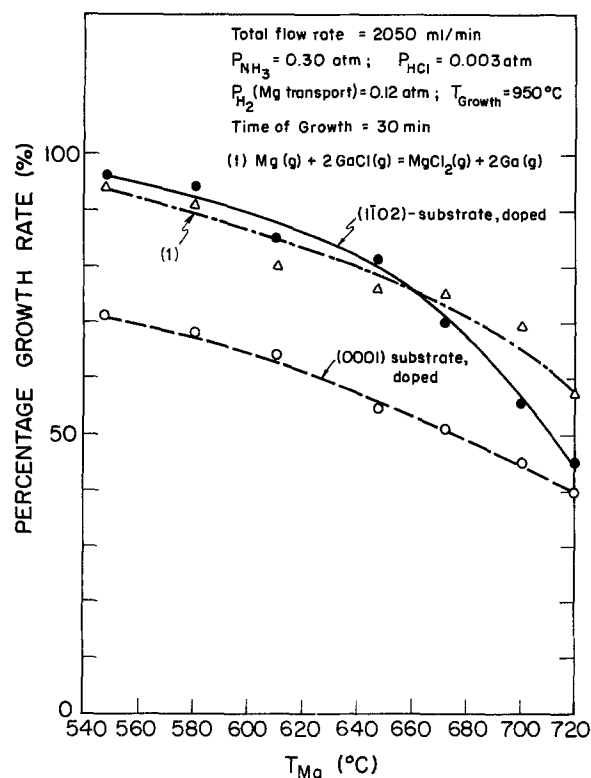


Fig. 13. Plot of percentage growth rate (with respect to the undoped) for doped GaN layer vs. Mg source temperature.

the catalytic effect of graphite confirmed (24). (This latter work, which measures the  $\text{NH}_3$  concentrations at individual points, should be contrasted to the integral effects obtained in the previous studies and in the present work.) Our results of the modest catalytic effect of quartz and graphite for the decomposition of  $\text{NH}_3$  are thus in agreement with the present literature.

Our significant finding, however, concerns the more pronounced enhancement of  $\text{NH}_3$  decomposition with the coexistence of Ga-GaN above a threshold temperature. The need for the coexistence of both Ga and GaN clearly implies a critical interaction between the two components. This is analogous to the interaction between metal and support in the case of supported-metal catalysts (25, 26) except that there is no clear definition of which component plays the role of support in the present case. Two types of interaction might be possible: either a "bifunctional" catalyst (27) in which one reaction occurs on one component to yield an intermediate product which further reacts on the other component, with neither one capable of producing the enhanced effect alone, or a modification of the chemical properties of one of the components at the interface (28). For the latter case, the enhancement might be caused by a modification of one or more of the following at the interface: the electronegativity of the metal, the surface composition, and the surface structure. There is no clear evidence to allow an evaluation of the relative merits of possible mechanisms and detailed account of catalytic mechanisms is beyond the scope of this study.

The implications of these results are obvious. Since several runs are made in succession in the same reaction zone in a typical growth system, the treatment of this zone between runs will clearly influence the basic driving force for the deposition reaction, particularly in the early stages of the deposition. Furthermore, the early stage of the deposition is critical since the initial nucleation will have a pronounced influence on the deposition in general. It was found that the morphology of the GaN is changed if GaN is grown in the presence of coexisting Ga-GaN as would be expected from the decrease in the affinity for the reaction that results from the  $\text{NH}_3$  decomposition. Another example

is the procedure established to improve the microstructure for GaN light emitting diodes by use of higher affinities at the early stage of growth. This was achieved by the use of Ar gas instead of  $\text{H}_2$  gas as a carrier gas (29). Furthermore, if nitrogen vacancies are the dominant donors in GaN that are responsible for the large intrinsic electron concentration, their concentration would be expected to vary with a change in the chemical potential of nitrogen which is clearly a function of the  $\text{NH}_3/\text{H}_2$  ratio. Obviously, in cases where one wishes to maximize the affinity of a reaction involving nitrogen as a reactant, one should avoid conditions conducive to the decomposition of  $\text{NH}_3$ . The general concept of catalytic potency of the reactor environment will certainly be important for other CVD processes, such as the synthesis of GaAs and GaP, especially when  $\text{NH}_3$  is used as a dopant.

**Growth kinetics.**—The experimental observations concerning the growth rate of GaN heteroepitaxial layers can be summarized as follows: (i) the growth rate is constant with respect to time; (ii) the growth rate decreases with increasing temperature within the temperature range of  $850^\circ\text{--}1150^\circ\text{C}$ ; (iii) the growth rate increases with increased flow rate of  $\text{NH}_3$  and/or  $\text{HCl}$ , and generally saturates; (iv) the growth rate is a function of the substrate position in the gas stream, it decreases as the substrate position is moved further downstream; (v) the growth rate depends on the catalytic nature of the growth environment and decreases under conditions of greater  $\text{NH}_3$  decomposition; (vi) the growth rate is significantly more rapid on R-plane substrates as compared to basal-plane substrates; (vii) the concurrent incorporation of Mg in the deposit, produced by the presence of Mg vapor in the growth zone, decreases the growth rate substantially.

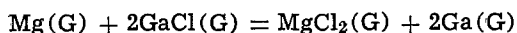
The temperature dependence of the growth rate is an apparent contradiction to predictions based on thermodynamics, as illustrated in Fig. 3 and 4. Since, in the majority of the growth runs studied, the extent of  $\text{NH}_3$  decomposition in the bulk stream was less than 10%, one would predict an increase in the equilibrium extent of reaction with increasing temperature in the temperature range studied. One would also expect the relative attainment of equilibrium to increase with increasing temperature since the detailed kinetic processes involved should be enhanced with increasing temperature. This apparent contradiction may be the result of a combination of two or more factors: inaccurate literature values for the thermodynamic data and the discrepancy between the bulk extent of decomposition of  $\text{NH}_3$  and the local extent of decomposition in the vicinity of the reaction interface. The weakest factor in the development of the thermodynamics of the deposition reaction is the standard Gibbs free energy of formation for GaN (15). These values were estimated since direct measurements of the standard enthalpy of formation, entropies, and heat capacities are not available at present. Thus, a discrepancy in the values that would displace the maximum in the curves in Fig. 3 and 4 downward by  $\sim 250^\circ\text{K}$  is not an unreasonable expectation. Furthermore, it must be noted that the extent of decomposition of  $\text{NH}_3$  that was experimentally determined in the present study was an integrated effect. It is possible and indeed probable, based on the recent work of Sedgwick (24), that the local extent of decomposition would shift the maxima in these curves to lower temperatures. It is obvious that in nonuniform reacting systems, such as CVD reactors, an *in situ* analysis technique for composition and temperature, with fine space resolution, is necessary to rigorously establish the thermodynamics near an interface.

The relative importance of two rate-limiting mechanisms in the epitaxial growth, mass transfer and surface reaction, cannot be clearly established for the present CVD system, but there is some evidence that it is a mixed controlled case. While there is a definite dependence of growth rate on the substrate and crys-



tal orientation (item vi), an observation commonly used to imply the existence of a surface reaction-controlled process, there is a dependence on the rate of supply of the reactants (items iii through v), commonly associated with mass transfer control mechanism. It is certainly clear that the reaction is not surface catalyzed since the deposition is not restricted to a definite surface and nucleation is easily accomplished. (These two conclusions are based on the fact that the deposition of GaN is not surface sensitive; for conditions used in typical growths, polycrystalline GaN can be deposited on practically any surface in the growth chamber, such as the fine textured Grafoil liner and fused quartz substrate holder.) It appears that there may be a homogeneous reaction producing a precursor for the GaN deposit. Indeed, in the presence of steep temperature gradients, noncoalescent randomly oriented GaN clusters appear on single crystal sapphire substrates and, for extreme conditions, ultra-fine powders ( $\sim 100\text{\AA}$ ) of GaN are formed (30).

The pronounced decrease in the growth rate caused by Mg doping, as illustrated in Fig. 13, might arise for two reasons: the displacement reaction between Mg and GaCl to produce a less reactive source of Ga, and the poisoning of the growth surface by the adsorption of Mg or MgCl. The Gibbs free energy of formation of GaCl is about  $-35$  kcal/mole at the growth temperature (21), whereas it is  $-110$  kcal/mole for  $\text{MgCl}_2$  (22). Thus the displacement reaction



should be complete in the vapor, if kinetic factors are favorable. From the geometrical configuration of the growth reactor (Fig. 1) the reaction will take place between the sidearm entrance and the  $\text{NH}_3$  inlet tube; thus, GaCl will be depleted before mixing with  $\text{NH}_3$ . Since in the growth of insulating layers, it is necessary to have a partial pressure of Mg that is 10-20% of the value for the partial pressure of GaCl in order to fully compensate the native donors in GaN, the depletion of the GaCl concentration due to this reaction can be significant.

One may calculate the decrease in the growth rate due to the addition of Mg, making the assumption that the above reaction goes to completion and that the reduced Ga does not react to form GaN. Comparison of such calculations with observations for the R-plane substrates (Fig. 13) shows good agreement at lower Mg concentrations, whereas the actual growth rate is depressed even further at Mg concentrations corresponding to full electrical compensation. This implies a surface poisoning effect at these higher concentrations, in addition to the depletion effect. It is also noticed in this regime of Mg concentration that there is a change in the surface morphology (31), as might be expected for a surface poisoning effect. The proposed surface poisoning effect correlates to a detrimental change in the substrate surface. This change may be caused either by a high Mg concentration in the lattice inducing a change in the GaN layer surface morphology or the presence of adsorbed Mg species on the growth surface. For growth on the basal plane, a pronounced effect was observed even at low Mg source temperatures, which is consistent with our observation that surface morphologies are altered with low Mg concentration for the basal-plane substrate (31).

### Summary

The nature of the growth ambient in the chemical vapor deposition of GaN was found to influence the extent of  $\text{NH}_3$  decomposition. Pure quartz, graphite, and GaN surfaces had a minor influence on the decomposition (up to a maximum of  $\sim 10\%$ ) whereas the coexistence of Ga and GaN caused extensive decomposition (up to  $\sim 60\%$ ) for the temperature range of  $950^\circ\text{--}1050^\circ\text{C}$ . The catalytic effect of the growth environment is thus a significant variable when  $\text{NH}_3$  is used as a reactant or dopant in chemical vapor deposition processes.

Several significant trends in the growth rate of GaN are reported for typical growth conditions: (i) The growth rate is linear with time. (ii) The growth rate decreases with increasing temperature, in the range  $850^\circ\text{--}1150^\circ\text{C}$ . (iii) The growth rate increases with increasing reactant composition. (iv) The growth rate decreases as the substrate is located further downstream. (v) The growth rate decreases when the growth environment favors the catalytic decomposition of  $\text{NH}_3$ . (vi) The growth rate is more rapid on R-plane sapphire substrates than on basal plane sapphire substrates. (vii) The growth rate decreases substantially when Mg is concurrently incorporated in the deposit.

An apparent discrepancy between the temperature dependence of the growth rate and the Gibbs free energy is noted and it is postulated that the discrepancy arises from local variations in  $\text{NH}_3$  concentration caused by decomposition and/or by incorrect thermodynamic data for the reactant species.

Manuscript submitted Nov. 30, 1977; revised manuscript received March 1, 1978.

Any discussion of this paper will appear in a Discussion Section to be published in the June 1979 JOURNAL. All discussions for the June 1979 Discussion Section should be submitted by Feb. 1, 1979.

Publication costs of this article were assisted by Intel Corporation.

### REFERENCES

1. H. P. Maruska, Ph.D. Thesis, Stanford University (1973).
2. T. L. Chu, *This Journal*, **118**, 1200 (1971).
3. H. P. Maruska and J. J. Tietjen, *Appl. Phys. Lett.*, **15**, 327 (1969).
4. H. M. Manasevit, F. M. Erdmann, and W. I. Simpson, *This Journal*, **118**, 1864 (1971).
5. J. J. Hsieh, Ph.D. Thesis, University of Southern California (1971).
6. R. Dingle, D. D. Sell, S. E. Stokowski, P. J. Dean, and R. B. Zetterstrom, *Phys. Rev. B*, **3**, 497 (1971).
7. R. Dingle and M. Ilegems, *Solid State Commun.*, **9**, 175 (1971).
8. A. Rabenau, "Compound Semiconductors," Vol. 1, chap. 19, Reinhold, New York (1962).
9. M. Ilegems and H. C. Montgomery, *J. Phys. Chem. Solids*, **34**, 885 (1973).
10. J. I. Pankove, E. A. Miller, and J. E. Berkeyheiser, *J. Lumin.*, **5**, 84 (1972).
11. J. I. Pankove, E. A. Miller, and J. E. Berkeyheiser, *RCA Rev.*, **32**, 383 (1971).
12. J. I. Pankove, E. A. Miller, and J. E. Berkeyheiser, *J. Lumin.*, **6**, 54 (1973).
13. H. P. Maruska, W. C. Rhines, and D. A. Stevenson, *Mater. Res. Bull.*, **7**, 777 (1972).
14. M. T. Duffy, C. C. Wang, G. D. O'Clock, Jr., S. H. McFarlane III, and D. J. Zanzucchi, *J. Electron. Mater.*, **2**, 359 (1973).
15. C. D. Thurmond and R. A. Logan, *This Journal*, **119**, 622 (1972).
16. J. B. MacChesney, P. M. Bridenbaugh, and P. B. O'Conner, *Mater. Res. Bull.*, **5**, 783 (1970).
17. R. Groh, G. Gery, L. Bartha, and J. I. Pankove, *Phys. Status Solidi A*, **26**, 353 (1974).
18. Y. Morimoto, *This Journal*, **121**, 1383 (1974).
19. A. G. Fischer, *Solid State Electron.*, **2**, 232 (1961).
20. V. S. Ban, *This Journal*, **119**, 761 (1972).
21. D. J. Kirwan, *ibid.*, **117**, 1572 (1970).
22. D. R. Stull, "JANAF Thermochemical Tables," (1967).
23. D. D. Roccasecca, R. H. Saul, and O. G. Lorimor, *This Journal*, **121**, 962 (1974).
24. T. O. Sedgwick and J. E. Smith, Jr., *ibid.*, **123**, 254 (1976).
25. M. Boudart, *Adv. Catalysis*, **20**, 153 (1969).
26. A. D. O. Cinneide and J. K. A. Clarke, *Catalysis Rev.*, **7**, (2), 213 (1972).
27. J. H. Sinfelt, *Adv. Chem. Eng.*, **5**, 37 (1964).
28. G. M. Schwab, *Discuss. Faraday Soc.*, **41**, 252 (1966).
29. G. Jacob, R. Madar, and J. Hallais, *Mater. Res. Bull.*, **11**, 445 (1976).
30. F. Q. Johnson and D. A. Stevenson, To be published.
31. S. S. Liu, T. L. Cass, and D. A. Stevenson, To be published.